ARTICLE

JAAS
www.rsc.org/jaas

A microwave assisted desolvation system based on the use of a TM_{010} cavity for inductively coupled plasma based analytical techniques

Guillermo Grindlay, Salvador Maestre, Juan Mora, Vicente Hernandis and Luis Gras*

Department of Analytical Chemistry, Nutrition and Food Sciences, University of Alicante, P.O. Box 99, 03080 Alicante, Spain. E-mail: luis.gras@ua.es

Received 6th December 2004, Accepted 9th March 2005
First published as an Advance Article on the web 29th March 2005

A new microwave assisted desolvation system based on the use of a TM_{010} cavity (MWDS2) has been developed and evaluated in plasma based analytical techniques: inductively coupled plasma atomic emission spectrometry (ICP-AES) and inductively coupled plasma mass spectrometry (ICP-MS). The new design overcomes the main experimental drawbacks shown by previous designs based on the use of domestic ovens: (i) lack of control on microwave generation and application; and (ii) inappropriate MW cavity characteristics. The evaluation has been performed in terms of the effect of the incident microwave power and the sample uptake rate and the results obtained has been compared with those afforded by a conventional sample introduction system (nebulizer and double pass spray chamber) and a desolvation system based on the use of a domestic microwave oven (MWDS). The new MWDS2 give rise to higher analytical signals and lower limits of detection and stabilization times (2–3 times) than those obtained with the MWDS in ICP-AES and ICP-MS.

Introduction

Aerosol desolvation is a well known method for overcoming spectral and non-spectral interferences caused by the presence of solvent in the atomization/ionization cell and for improving the analyte transport rate when introducing liquid samples in inductively coupled plasma techniques (ICP-AES and ICP-MS).

In general, desolvation systems can be divided in two groups: those which employ a single step (usually a thermostated spray chamber) and those which employ a heating step for improving solvent vaporization followed by a vapour removal step. In the first case only solvent load reduction is possible, whereas when using two-step desolvation systems the analyte transport rate is also increased.[1] Different heat sources have been employed for aerosol vaporization. Among them, the most common is to keep the walls of the spray chamber at high temperature (a few degrees over solvent boiling point) by means of a heating tape wound around it.[2,3] Aerosol radiative heating has also been used. These devices are, in general, more efficient than conductive heating ones and reduce some of the drawbacks shown by the latter. IR[4] or UV-vis[5] have been used to this end. During the last years microwave radiation has also been employed for aerosol desolvation by means of the so-called microwave desolvation system (MWDS).[6–9] This system provides, with plain water solutions, higher analytical signals than a conventional sample introduction system (CS) made up by a double-pass spray chamber.[6] Nevertheless, owing to the characteristics of the microwave heating, the analytical behaviour of the MWDS strongly depends on the nature and matrix of the sample.[7] Thus, in ICP-AES, 0.1 mol l^{-1} solutions of sulfuric and perchloric acid give rise to signals that are five and four times higher, respectively, than those obtained using plain water alone. Desolvation of acid solutions by IR radiation was also studied and matrix effects compared with those previously obtained with the MWDS. The results showed that the MWDS is more prone than IRDS to matrix effects due to sulfuric or perchloric acid, but the limits of detection obtained with both systems are similar.[8]

In ICP-MS the MWDS provides ion intensities between 2 and 14 times higher then those obtained with a CS, whereas RSD values are similar (<3%). For isotopes not affected by spectral interference, LODs obtained with the MWDS are up to ten times lower than those obtained with the CS.[9]

In spite of the promising results obtained with the MWDS, the system shows some drawbacks derived from an inefficient heating process as a consequence of the use of a domestic oven. In general, for an efficient microwave heating it is necessary to design a specific cavity for each application (spray chamber, material or sample). Hence, for aerosol desolvation, appropriate MW cavity design might improve the results obtained with previous designs. Monomode microwave cavities have been employed in several analytical applications such as: sample treatment,[10] aerosol nebulization (MWTN)[11] and plasma generation (MIP).[12] Among the different monomode cavity types the TM_{010} shows several characteristics that *a priori* made it appropriate for aerosol heating.[13]

The aim of the present work is to develop a new heating step of a microwave based desolvation system using a TM_{010} cavity and to evaluate its analytical figures of merit in ICP-AES and ICP-MS.

Experimental

Sample introduction system

The drawbacks shown by the MWDS and mentioned above can be divided in two groups: (1) those related to microwave generation and application (lack of control on the incident and reflected microwave power); and (2) those related to cavity properties. These last could be: (i) inappropriate spray chamber design (shape and dimensions); (ii) existence of large aerosol conductions inside the MW cavity (more than 30 cm length); and (iii) the use of a multi-mode cavity, since the configuration of a domestic oven forces one to place the nebulizer, and hence the spray chamber, in a specific position (the hole placed at the centre of the oven bottom is employed for introducing the nebulizer) that does not always coincide

DOI: 10.1039/b418282k

with the position of maximum microwave energy. For instance, Fig. 1 shows the energy pattern distribution, measured according a procedure proposed by Kingston,[14] of two different domestic ovens: that employed in the MWDS (Model W-2235, Balay, Zaragoza, Spain) and other of similar dimensions and power (Model M9235, Samsung, Barcelona, Spain) Fig. 1A and 1B, respectively. As can be seen in this figure, the cavity employed in the MWDS shows a maximum in the centre, whereas in the other one the maximum is located near to the right border of the cavity. Hence, the cavity shown in Fig. 1B is inappropriate for an efficient aerosol heating, since the aerosol vaporization achieved is lower than with the MWDS.

On the contrary, as has also been previously mentioned, the TM_{010} cavity shows several characteristics that *a priori* make it appropriate for aerosol heating:[13] (i) the energy distribution pattern is well known and the spray chamber can be placed in the maximum energy position; (ii) by mechanizing the spray chamber with suitable dimensions, practically all its inner volume is placed within a strong microwave field while keeping the walls out of the irradiated zone; (iii) the cavity properties can be modified by using tuning screws for achieving the maximum interaction between the aerosol and the electromagnetic field;[15] and (iv) it is also possible to make small holes in the cavity without microwave leakage.

It is also worth noting that, for a precise incident and reflected microwave power control, it is necessary to employ a variable microwave source and a waveguide configuration that allows the inclusion of a power-meter for reflected energy measurements.

Fig. 2 shows the experimental setup of the new microwave desolvation system, hereinafter called MWDS2, the axial view of the cavity and the calculated electrical field (Fig. 2A–2C, respectively). The aerosol generated by the pneumatic concentric nebulizer (1) (Model TR-30-A3, Meinhard, Santa Ana, CA, USA) is introduced in a quartz spray chamber (2) (inner volume, 52 cm^3), vertically placed at the centre of a TM_{010} cavity (3). Microwave cavity dimensions were calculated so as to obtain a maximum microwave field in the volume occupied by the spray chamber. The cavity has a cylindrical adjustable insertion (tuning screw) (4) placed in the centre of the cavity (maximum electric field) for maintaining the resonance frequency at (or near) the nominal magnetron resonance frequency. The distance between the tuning screw and the cavity

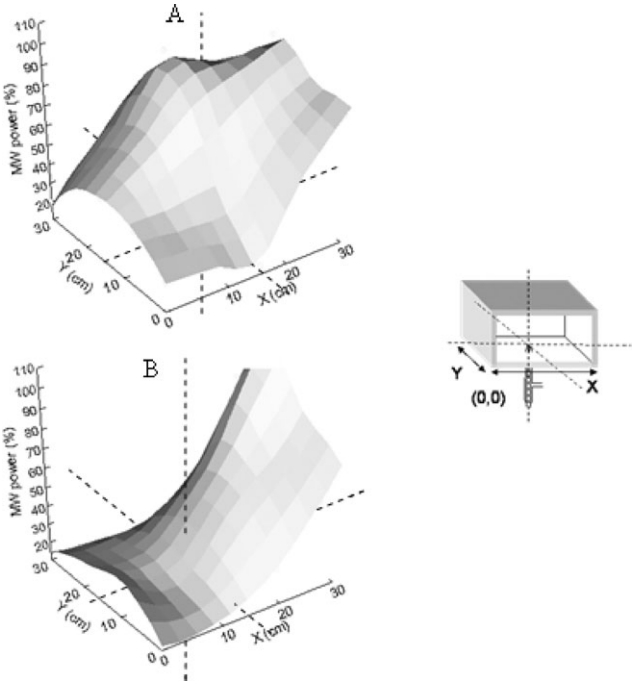

Fig. 1 Energy pattern distribution inside the cavity of two different domestic ovens operating at the same nominal power (see text for explanation).

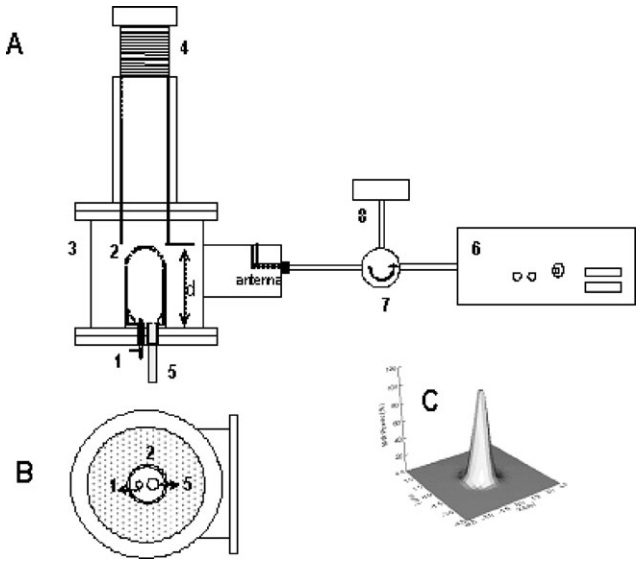

Fig. 2 (A) Experimental setup of the MWDS2. (1) Nebulizer; (2) spray chamber; (3) TM_{010} microwave cavity; (4) tuning screw; (5) aerosol exit and spray chamber drain; (6) magnetron; (7) circulator; (8) dummy load. (B) Axial view of the microwave cavity. (C) Energy pattern distribution (calculated) inside the TM_{010} microwave cavity.

bottom (d in Fig. 2A) represents the distance between two capacitor plates. As the screw is moved in, the distance between the two plates becomes smaller and the capacitance increases. This increase in capacitance causes a decrease in the resonant frequency. As the screw is moved out, the resonant frequency of the cavity increases. The spray chamber aerosol exit is located at the spray chamber bottom, close to the nebulizer, and is also employed as drain (5). Hence, no additional tubes are needed for the aerosol leaving the spray chamber. Microwaves are generated by means of a magnetron (6) of 2.45 GHz (Model GMP 03 K/SM, Sairem S. A., Neyron, France), with a power of 300 W and connected with the cavity by a coaxial line. This device allows precise incident microwave power control because the supplied power can be smoothly modified (without time chopping) in steps of 1 W. A safety device for monitoring the reflected radiation, made up of a circulator (7) and a dummy load (8) equipped with a power-meter, is placed between the generator and the cavity. Using this configuration MW power absorbed inside the cavity can be measured as the difference between incident and reflected power. The vapour removing step has been previously employed in the MWDS and consists of two Liebig condensers placed in series at 10 and −1 °C, respectively.

The sample uptake rate (Q_l) was controlled by means of a peristaltic pump (Model Minipulse 3, Gilson, Villiers-Le-Bel, France) and the nebulizer gas flow rate (Q_g) by means of a calibrated flowmeter (Cole-Palmer Inc., Chicago, IL, USA).

Table 1 shows the characteristics of the two microwave based sample introduction systems developed by our group and tested in the present work (MWDS and MWDS2).

For the sake of comparison, two conventional sample introduction systems were employed. In ICP-AES, a concentric nebulizer (Meihard TR-30-A3) and a Ryton double pass spray chamber (100 cm^3 inner volume) were used, whereas for ICP-MS the sample introduction system employed was the standard one supplied with the instrument, made up of a Conikal nebulizer (AR-30-1F3E, Glass Expansion, Hawthorn, Victoria, Australia) and a thermostated (5 °C) single pass spray chamber with impact bead.

Analyte transport measurements

Analyte transport rate (W_{tot}) measurements were performed by nebulizing a solution of 500 μg Mn L^{-1} during a given period

Table 1 Characteristics of the two microwave sample introduction systems tested

	Characteristics	
	MWDS	MWDS2
Cavity	Multimode	Single mode (TM_{010})
MW generator	Pulse	Continuous
Safety device	No	Yes
Incident power	Fixed	0–300 W
Reflected MW power	Unknown	0–20 W

of time and trapping the aerosol at the exit either of the desolvation system (MWDS and MWDS2) or of the spray chamber (CS) with a glass fibre filter (type A/E, 47 mm diameter, 0.3 μm pore size, Gelman Sciences, Ann Arbor, MI, USA). The filter was then washed out into a volumetric flask with 1.0% (w/w) nitric acid. The manganese content in each flask was measured by flame atomic absorption spectrometry. A set of three replicates was performed in each case, being the RSD of these measurements lower than 4%.

ICP instrumentation

ICP-AES measurements were made using a PerkinElmer Optima 3000 ICP-AES system (PerkinElmer, Uberlingen, Germany). A VG PQ Excell CCT instrument (ThermoElemental, Winsford, Cheshire, UK) was used for ICP-MS measurements. Table 2 shows the operating conditions of the ICP-AES and ICP-MS instruments.

Reagents and samples

All chemicals employed were of analytical grade. Test solutions containing 1 μg ml^{-1} for ICP-AES or 10 ng ml^{-1} for ICP-MS measurements were prepared by diluting appropriate aliquots of 1000 μg ml^{-1} multielemental reference solutions (Merck, Darmstadt, Germany). Analytical lines of elements covering a wide range of E_{sum}, defined as the sum of excitation and ionization energies, in ICP-AES and m/z values in ICP-MS were selected (see Table 3).

Table 2 Operating conditions of the ICP-AES and ICP-MS instruments

PerkinElmer Optima 3000 ICP-AES	
Plasma forward power/W	1450
Argon flow rate/l min^{-1}:	
Plasma	15
Auxiliary	0.5
Nebulizer	0.6[a]–0.7[b]
Sample uptake rate/μl min^{-1}	Variable
Observation height/mm ALC	5[a]–10[b]
Inner tube diameter/mm	0.8

VG PQ-Excell CCT ICP-MS	
Plasma forward power/W	1450
Argon flow rate/l min^{-1}:	
Plasma	13
Auxiliary	1
Nebulizer	Variable
Sample uptake rate/μl min^{-1}	Variable
Scanning mode	Peak hopping
Points per peak	3
Dwell time/μs	500
Number of sweeps	30

[a] SC and SDMW. [b] MWDS2.

Table 3 Analytical lines of elements with their exication and ionization energies, as well as m/z values of isotopes investigated

	ICP-AES		ICP-MS	
Elements	Wavelenght/nm (line type)	E_{sum}/eV[a]	m/z	E_{ion}/eV
Li	—	—	7	5.39
Be	—	—	9	9.32
Mg	285.213 (I)	4.35	—	
	280.270 (II)	12.07		7.64
Al	396.152 (I)	3.14	27	5.96
Ar	420.068 (I)	3.95	—	—
Sc	—	—	45	6.54
Cr	267.710 (II)	12.92	—	—
Mn	257.610 (II)	12.29	55	7.43
Fe	238.204 (II)	13.07	56	7.87
Co	228.616 (II)	13.70	59	7.86
Cu	324.754 (II)	3.82	63	7.72
Ni	221.647 (II)	14.03	—	—
Cd	—	—	111	8.99
In	—	—	115	5.79
Ba	455.403 (I)	7.93	138	5.21
Ce	—	—	140	5.6
Pb	220.353 (II)	14.79	208	7.42
U	—	—	238	6.08

[a] $E_{sum} = E_{exc} + E_{ion}$.

Results and discussion

Fundamental studies

Fig. 3 shows the effect of the frequency on the cavity reflection coefficient, defined as the ratio of the amplitude of the reflected wave to the amplitude of the incident one, for different tuning screw positions in the presence and absence of aerosol. These measurements were performed, according to the D2520-95 American Society for Testing and Materials (ASTM) standard,[16] as follows: For a given tuning screw position (d value), the reflection coefficient was measured under dry conditions (*i.e.*, without water in the spray chamber). After that, aerosol was generated using plain water ($Q_l = 300$ μl min^{-1}) and the coefficient measured after 10 s without stopping nebulization. The spray chamber was removed and dried carefully between experiments.

The microwave power absorbed per unit volume by dielectric materials is given by eqn. (1):

$$P = 2\pi\nu\varepsilon_0\varepsilon'' E_i^2 \quad (1)$$

where ν is the frequency (Hz); ε_0 the free space permittivity; ε'' the dielectric loss factor; and E_i the electric field inside dielectric material (V m^{-1}).

For an efficient power transfer in microwave cavities it is necessary to maintain the resonance frequency of the cavity within the fixed frequency band (typically 5–10 MHz wide) of the magnetron and to have a high energy density in the volume occupied by the irradiated material.

In general, insertion of dielectric materials into a microwave cavity causes the resonance frequency to decrease from the empty-cavity value.[13] Moreover, the electrical permittivities of most materials vary with temperature, leading to additional lowering of the resonance frequency during microwave heating.[17] Hence, cavity tuning is mandatory due to the de-tuning effect exerted by samples. In the case of the MWDS2 tuning is achieved by changing manually the position of the tuning screw (4 in Fig. 2) until reflected power reaches a minimum.

Results from Fig. 3 show that the presence of the aerosol exerts the typical de-tuning effect due to dielectric materials, thus proving the existence of aerosol–microwave coupling. Mie scattering theory has been employed by some authors for

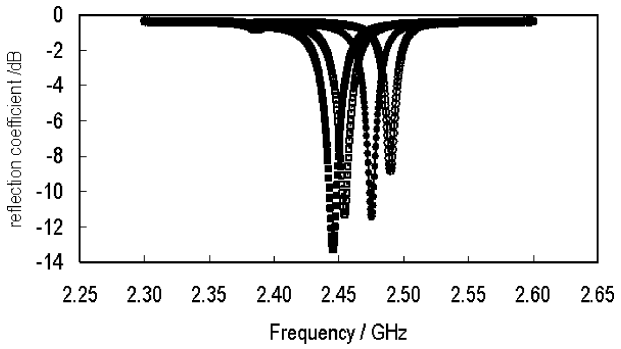

Fig. 3 Effect of the frequency on the cavity reflection coefficient for different tuning screw positions: (○) $d = 93.1$ mm without aerosol; (●) $d = 93.1$ mm with aerosol; (□) $d = 91.6$ mm without aerosol; (■) $d = 91.6$ mm with aerosol.

evaluating the microwave power absorbed by a single drop of water and for estimating drop heating and solvent vaporization.[18] These calculations conclude that vaporization of a single drop due to microwave heating is an inefficient process. Nevertheless, Fig. 3 shows that an aerosol confined inside a spray chamber interacts with a microwave field. The explanation of this different behaviour is not yet well understood, but seems to be related to the heterogeneity[19] and electrical properties of the aerosols (*i.e.*, charge distribution on droplet surface).

Data from Fig. 3 also allow the estimation of the so-called *quality factor of the cavity* (Q). This factor is inversely related to the dielectric loss factor (ε'') and hence to the heating capability of the irradiated system. Q values were calculated using the full width of the half minimum band (FWHM) and following the ASTM recommendations (eqn. (2)).[16]

$$Q = \frac{\mathrm{FWHM}}{\nu_{\min}} = \frac{1}{tg\delta} = \frac{1}{tg\frac{\varepsilon''}{\varepsilon'}} \qquad (2)$$

In general, a reduction in Q means a more efficient heating process. Calculated Q values in the presence of aerosol were 32 and 16% lower than those obtained in the absence of aerosol for d values of 91.6 and 93.1 mm, respectively, thus supporting the existence of aerosol heating by microwaves. Data also reveal that the insertion of the tuning screw around 91.6 mm gives rise to a cavity frequency resonance close to 2.45 GHz (the nominal frequency of the magnetron). For this reason, the rest of measurements were performed by optimizing the tuning screw position around this value.

ICP-AES

Effect of the incident microwave power. Fig. 4 shows the effect of the nominal incident microwave power on the manganese normalized net emission intensity obtained in ICP-AES (I_{nor}) for different Q_{l} values. The results in Fig. 4 show that an increase in the power causes I_{nor} to increase for all Q_{l} tested. According to eqn. (1), this is the expected behaviour since solvent vaporization, and hence analyte transport rate, increases when the electromagnetic field intensity inside the cavity is increased. It is important to remark that the reflected power is always lower than 20 W (on average 15 W). This means that, with appropriate cavity tuning, the higher the incident power the higher the power absorbed by the irradiated system.

Effect of sample uptake rate. Fig. 5 shows the effect of Q_{l} on the normalized net line intensity of manganese obtained with all the sample introduction systems tested. When comparing the emission signals obtained with the three different systems, results point out that, as expected, both desolvation systems afford higher signals than the CS at any of the Q_{l} values tested. When comparing MWDS and MWDS2 it is clear that the MWDS2 gives rise to higher manganese emission signals (up to 7 times) and also a different behaviour between both systems becomes apparent on increasing Q_{l}. When using the MWDS2 an increase in Q_{l} gives rise to a continuous increase in I_{nor} as a consequence of an increase in W_{tot}, whereas with the MWDS a maximum appears at 100 μl min^{-1}. It is worth noting that the MWDS2 also shows a maximum when using low incident powers (*i.e.*, 50, 100 or 150 W). When using desolvation systems, the existence of a maximum in emission intensity when increasing Q_{l} is directly related to the vaporization capability of the heating step. Although the power supplied by the MWDS (790 W) is higher than that supplied by the MWDS2 (290 W), the higher energy transfer efficiency achieved by the latter because of the improved cavity design will increase solvent vaporization, analyte transport rate and analytical signal. This hypothesis is confirmed by the aerosol transport measurements. Thus, at 400 μl min^{-1} the W_{tot} value obtained with the MWDS2 is higher (about 15 times higher) than that obtained with the CS, whereas the MWDS affords intermediate values.

Fig. 6 shows the effect of analyte E_{sum} on the relative net intensity (I_{rel}) obtained at 100 and 400 μl min^{-1} with the three sample introduction systems used in the present work. I_{rel} has been defined as the ratio between the emission intensity obtained with the MWDS2 and the intensity obtained with an alternative system ($I_{\mathrm{rel}} = I_{\mathrm{MWDS2}}/I_{\mathrm{CS}}$ or $I_{\mathrm{rel}} = I_{\mathrm{MWDS2}}/I_{\mathrm{MWDS}}$). The results shown in Fig. 6 indicate that no significant differences can be found between the MWDS and MWDS2 at 100 μl min^{-1} ($I_{\mathrm{rel}} \approx 1$). Nevertheless, at 400 μl min^{-1}, I_{rel} values obtained with the MWDS2 are always higher than those obtained with the MWDS (6.9 times on average). When comparing CS and MWDS2, I_{rel} values are always higher than 1 (up to 34 times) and also higher than those obtained with MWDS at the same Q_{l}. This situation is related to the behaviour observed in Fig. 5 and is a direct consequence of the higher W_{tot} values achieved with the MWDS2. Results also indicate that, in general, an increase in E_{sum} produces a

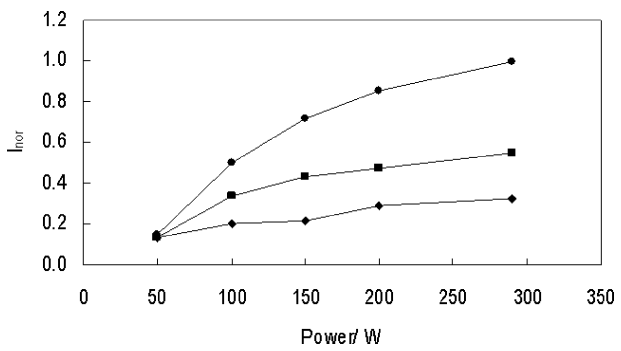

Fig. 4 Effect of nominal incident microwave power on the normalized net emission intensity of Mn 257.610 nm at different sample uptake rates: (◆) 50 μl min^{-1}; (■) 100 μl min^{-1}; (●) 200 μl min^{-1}.

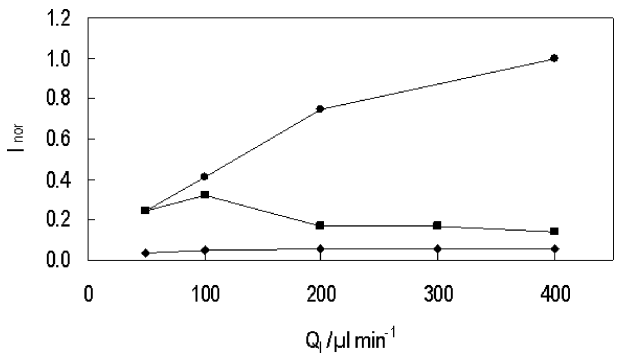

Fig. 5 Effect of sample uptake rate on the normalized net line intensity of Mn 257.610 applying (◆) conventional, (■) MWDS 790 W and (●) MWDS2 290 W sample introduction system.

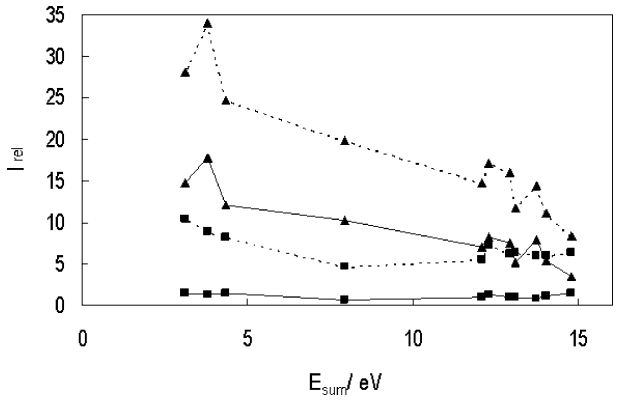

Fig. 6 Relative intensities of analytical lines of elements investigated in function of E_{sum}, determined at sample uptake rate of 100 μl min^{-1} (continuous lines) and 400 μl min^{-1} (dotted lines): (■) MWDS2/MWDS; (▲) MWDS2/CS.

decrease in I_{rel}. This behaviour can be explained by taking into account that lines with higher E_{sum} are more influenced by the presence of solvent in the plasma. It is well known that for E_{sum} values lower than 5.1 eV the presence of solvent does not significantly modifiy the emission intensity, whereas for higher E_{sum} values the emission intensity decreases when S_{tot} is increased.[20]

The plasma solvent load was estimated by measuring the OH emission band (309.311 nm), whereas the plasma excitation conditions were measured by the Mg ionic to atomic emission intensity ratio (Mg II/Mg I). The OH band signal remains constant as Q_l is increased for the three systems tested, the values obtained with the MWDS2 being 1.7 and 1.3 times higher than those obtained with the CS and MWDS, respectively. The results indicate that more solvent is introduced into the plasma when using both microwave based desolvation systems and also that the more efficient the heating step, the higher the solvent transport. These results can be explained by taking into account that the increase in solvent vapour achieved as a consequence of a more efficient heating process is not efficiently removed from the aerosol stream by the vapour removing step employed. However, the amount of solvent reaching the plasma is not high enough for changing significantly its excitation conditions. Thus, the Mg II/Mg I ratio, as happens with the OH band, remains unchanged when Q_l is increased. The Mg II/Mg I ratios obtained with the MWDS2 are about half those obtained with the CS. The different behaviour observed for W_{tot} and the estimated plasma solvent load when increasing Q_l can be explained bearing in mind that the solvent transport rate, and hence the plasma solvent load, increases to a lesser extent than W_{tot} does when using desolvation systems.[1,21] The parameters employed reflect correctly the behavior of S_{tot} when comparing introduction systems, but they do not have enough sensitivity for reflecting the small changes produced in S_{tot} when increasing the solvent uptake rate in a desolvation system.

The reduction observed in the intensity of analytical lines with high E_{sum} when using any of the microwave based desolvation systems is related to the amount of solvent reaching the plasma and explains why the reduction in I_{rel} observed with the MWDS is lower than that observed with the CS. As a consequence, it seems to be clear that, when using a highly efficient solvent vaporization step, the use of an efficient vapour removal step is mandatory for adequate aerosol desolvation.

Stabilization and wash-out times

Stabilization time, defined as the time required for achieving a constant signal after switching on the microwave based systems, was evaluated. In both cases, the stabilization time decreases as Q_l is increased. Thus, for instance, the stabilization time for the MWDS2 goes from 600 to 300 s when Q_l is increased from 100 to 400 μl min^{-1}. When comparing the systems, the MWDS2 shows stabilization times 2–3 times lower than those obtained when using the MWDS, as a consequence of the improved efficiency of the cavity employed.

The wash-out time, defined as the time required for reaching 1% of the stable signal after blank introduction, shows a similar behaviour to that reported for the stabilization time, depending inversely on Q_l. Nevertheless, in this case both desolvation systems show similar wash out times (80 s at 400 ml min^{-1}) twice that obtained when using the CS. This parameter depends on the total volume of the sample introduction system and, in this case, no noticeable differences can be found between both desolvation systems.

Signal stability

The signal stability of the MWDS2 has been evaluated using two different parameters: RSD and long term stability. As regards RSD, the MWDS2 provides values about 2–5%. These RSD are similar than those obtained with the MWDS and slightly higher than those with the CS (1–3%). Regarding the long term stability of the MWDS2, signal measurements during several hours have shown a precision better than 6%, whereas measurements of the same solution during a whole year have shown a signal reproducibility better than 10%.

Limits of detection

Table 4 shows the reduction in the LODs, calculated according the approach described by Boumans,[22–24] obtained with the microwave based systems compared with the CS (LOD_{CS}/LOD_{MW}) at 400 μl min^{-1} for different elements and their analytical lines shown in Table 3. As a consequence of the higher sensitivity (see Fig. 5), LODs obtained with the MWDS2 are up to 25 times lower than those with the CS. The differences in sensitivity shown in Fig. 5 also appear when comparing the LODs obtained with MWDS and MWDS2, since the RSD obtained in both cases are similar (< 5%). Thus, at 400 μl min^{-1}, the ratio LOD_{MWDS}/LOD_{MWDS2} is, on average, 6.2, whereas this ratio is 1.3 at 100 μl min^{-1}.

Table 4 Relative LOD values for different analytical lines and isotopes in ICP-AES and ICP-MS Q_I = 400 μl min^{-1}

	ICP-AES		ICP-MS
Elements	LOD_{CS}/LOD_{MWDS}	LOD_{CS}/LOD_{MWDS2}	LOD_{CS}/LOD_{MWDS2}
Li	—	—	8.2
Be	—	—	1.3
Mg I	3.2	25.2	—
Mg II	0.9	13.8	—
Al	4.0	20.8	3.3
Sc	—	—	1.5
Cr	2.6	11.4	—
Mn	0.5	15.3	4.1
Fe	2.9	12.1	4.9
Co	1.8	7.9	2.2
Cu	5.9	21.6	3.1
Ni	1.4	8.4	—
Cd	—	—	1.9
In	—	—	3.7
Ba	1.3	13.6	5.2
Ce	—	—	2.5
Pb	1.3	6.5	3.2
U	—	—	2.9

As regards the data shown in Table 4, and taking into account the E_{sum} values of Table 3, a noticeable effect of the E_{sum} on the LOD reduction can be observed. The higher the E_{sum} the lower the LOD reduction achieved. Thus, for instance when using the MWDS2, the E_{sum} of the Mg 285.213 line is 4.35 eV and shows a LOD reduction of 25 times; Fe 238.204 and Cr 267.595 with E_{sum} values of 13.07 and 12.92 eV, respectively, show similar reductions (around 12 times), whereas the line Pb 220.353 (E_{sum} = 14.79 eV) shows the lowest LOD reduction. This effect is in good agreement with data shown in Fig. 5 and is also related to the amount of solvent reaching the plasma.

ICP-MS

Effect of nebulizer gas flow rate. Fig. 7 shows the effect of the gas flow rate on the ^{115}In normalized signal (Fig. 7A) and the oxide level (CeO^+/Ce^+ ratio) (Fig. 7B) obtained with the MWDS2 and the sample introduction system provided with the instrument. The oxide level has been used for evaluating the modification of plasma conditions due to solvent load. In general, and as a consequence of its higher efficiency, the MWDS2 gives rise to higher signals than those obtained with the conventional sample introduction system. Fig. 7A also indicates that I_{nor} peaks at a lower Q_g for the MWDS2 than for the sample introduction system provided with the instrument. This behaviour can be explained by taking into account that a reduction in the optimum Q_g is related, in general, to an increase of the solvent load into the plasma. As has been previously stated, the MWDS2 affords higher values of the analyte and solvent transport rates than the conventional sample introduction system.

The oxide level values shown in Fig. 7B indicate that an increase in Q_g gives rise to a significant increase in the ratio that is directly related to the signal reduction observed in Fig. 7A. These results point out that a more efficient solvent removal step (lower condensation temperatures or vapor removal by membranes) is necessary for improving the signals obtained with the MWDS2 in ICP-MS.

Effect of sample uptake rate. Fig. 8 shows the effect of the sample uptake rate on the ^{115}In normalized signal (Fig. 8A) and the CeO^+/Ce^+ ratio (Fig. 8B) obtained with the MWDS2 and the CS provided with the instrument. Results shown in Fig. 8A indicate that, as a difference from that previously observed in ICP-AES (Fig. 5), when using the MWDS2 I_{nor} shows a maximum at 100 µl min^{-1}. This behaviour is different from that previously observed in emission because in ICP-AES the signal steadily increases as Q_l is increased. Again, this difference could be related to the presence of solvent in the plasma since solvent load increases with increase in Q_l. The oxide level results indicate that an increase in Q_l gives rise to a significant increase in the ratio that is directly related to the signal reduction observed in Fig. 8A as a consequence of the increase of the solvent load into the plasma.

As a consequence of the results shown in Figs. 7 and 8, it seems to be clear that a careful instrumental optimization is necessary to get the maximum signal increase due to the increased analyte transport rate afforded by the MWDS2. Under optimized instrumental parameters (Q_g = 1.0 l min^{-1}, Q_l = 100 µl min^{-1}), the MWDS2 gives, on average, a 13 times signal enhancement (similar to that obtained in ICP-AES) irrespective of the m/z value.

Limits of detection. Table 4 shows the LODs obtained with the MWDS2 when compared with the CS supplied with the instrument (LOD_{CS}/LOD_{MW}) at 100 µl min^{-1}. According to these results, LODs obtained with MWDS2 are lower than those obtained with the CS as a consequence of the higher sensitivity achieved with the former. On average, the reduction in LODs obtained with the MWDS2 is 3.4 times. This factor is lower than that expected according to the signal enhancement shown above (13 times). This fact cannot be explained by just taking into account the RSD, since these values are similar for both systems (on average, 3.3 and 4.5 for CS and MWDS2, respectively), but might be related to the increase in the background signals shown by the MWDS2. Thus, for instance, the signal for ^{56}Fe (which is interfered by the $^{56}ArO^+$ signal) is 16 times higher than that obtained with the CS, whereas the background is 4 times higher.

Finally, from the results shown in Table 4 and data gathered in Table 3, it can also be seen that no noticeable effect of E_{ion} or m/z value on the LODs is observed.

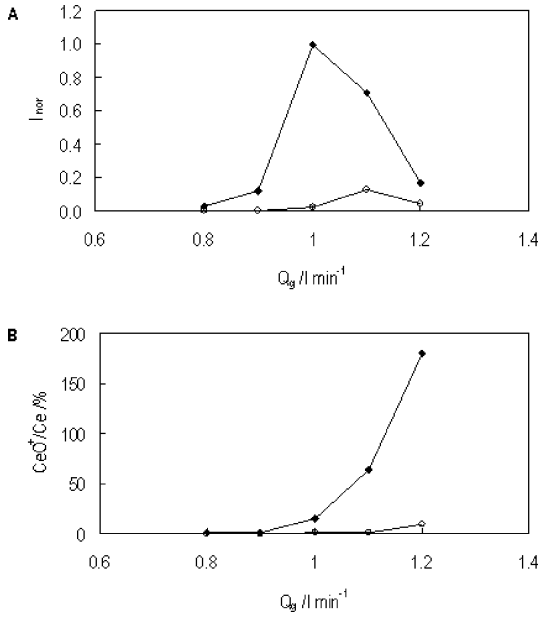

Fig. 7 Effect of nebulizer gas flow rate on the normalized ^{115}In signal (A) and on the CeO^+/Ce^+ ratio (B) obtained with ICP-MS. Q_l = 100 µl min^{-1}: (○) conventional sample introduction system; (◆) MWDS2, 290 W.

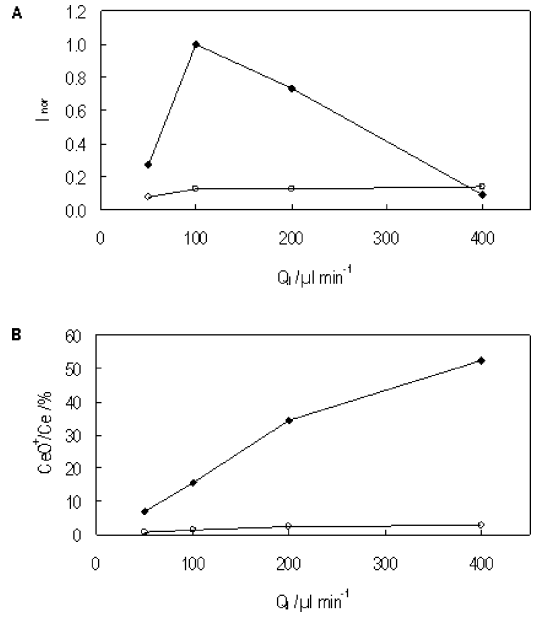

Fig. 8 Effect of sample uptake rate on the normalized ^{115}In signal (A) and on the CeO^+/Ce^+ ratio (B) obtained in ICP-MS. Q_g = optimum with each system. (○) Conventional sample introduction system; (◆) MWDS2, 290 W.

Conclusions

The microwave based sample introduction system presented in this work, which makes use of a TM_{010} cavity (MWDS2), overcomes the experimental drawbacks and improves the analytical behaviour shown by previous designs. The MWDS2 give rise to higher signals and lower LODs than those obtained with previous microwave based designs and conventional sample introduction systems in ICP-AES or ICP-MS.

Acknowledgements

The authors thank Dr. J. M. Catalá from the Deparment of Comunications of Universitat Politecnica de Valencia for his contribution in the design of the MW cavity. G. Grindlay also thanks the University of Alicante for the fellowship.

References

1 J. Mora, J. L. Todolí, I. Rico and A. Canals, *Analyst*, 1998, **123**, 1229.
2 A. R. Eastgate, R. C. Fry and G. H. Gower, *J. Anal. At. Spectrom.*, 1993, **8**, 305.
3 L. C. Alves, M. G. Minnich, D. R. Wiederin and R. S. Houk, *J. Anal. At. Spectrom.*, 1994, **9**, 399.
4 A. R. Eastgate and W. Vogel, Patent No WO 92/02282, 1992.
5 P. D. Goulden and D. H. Anthony, *Anal. Chem.*, 1982, **54**, 1678.
6 L. Gras, J. Mora, J. L. Todolí, V. Hernandis and A. Canals, *Spectrochim. Acta, Part B*, 1997, **52**, 1201.
7 L. Gras, J. Mora, J. L. Todolí, A. Canals and V. Hernandis, *Spectrochim. Acta, Part B*, 1999, **54**, 469.
8 L. Gras, J. Mora, J. L. Todolí, A. Canals and V. Hernandis, *Spectrochim. Acta, Part B*, 1999, **54**, 1321.
9 J. Mora, A. Canals, V. Hernandis, E. H. Van Veen and M. T. C. de Loos-Vollebregt, *J. Anal. At. Spectrom.*, 1999, **13**, 175.
10 *Microwave-enhanced Chemistry*, eds. H. M. Kingston and S. J. Haswell, American Chemical Society, 1997.
11 L. Ding, F. Liang, Y. Huan, Y. Cao, H. Zhang and Q. Jin, *J. Anal. At. Spectrom.*, 2000, **15**, 293.
12 *Inductively Coupled Plasma Mass Spectrometry*, ed. A. Montaser, Wiley-VCH, 1998.
13 A. C. Metaxas, *Foundations of Electroheat*, Wiley, 1996.
14 *Microwave Enhanced Chemistry (Chapter 2)*, eds. H. M. Kingston and S. J. Haswell, ACS, 1997.
15 Q. Jin, F. Liang, H. Zhang, L. Zhao, Y. Huan and D. Song, *Trends Anal. Chem.*, 1999, **18**, 479.
16 Test methods for complex permittivity (Dielectric Constant) of solid electrical insulating materials at microwave frequencies and temperatures to 1650 °C, ASTM Standard D 2520-95, American Society for Testing and Materials, 1995.
17 A. Zlotorzynski, *Crit. Rev. Anal. Chem.*, 1995, **25**, 43.
18 K. O. Douglass, N. Fitzgerald, B. J. Ingebrethsen and J. F. Tyson, *Spectrochim. Acta, Part B*, 2004, **59**, 261.
19 A. Canals, L. Gras, J. Mora, V. Hernandis, J. Margineda, M. Rojo and J. Muñoz, *Spectrochim. Acta, Part B*, 1999, **54**, 333.
20 D. E. Nixon, *J. Anal. At. Spectrom.*, 1990, **5**, 531.
21 H. A. Contreras, PhD Thesis, University of Alicante, Spain, 2001.
22 P. W. J. M. Boumans, *Spectrochim. Acta, Part B*, 1991, **46**, 431.
23 P. W. J. M. Boumans, *Spectrochim. Acta, Part B*, 1991, **46**, 917.
24 P. W. J. M. Boumans, *J. Anal. At. Spectrom.*, 1993, **8**, 767.